JOURNAL OF MATERIALS SCIENCE **40** (2005) 5635–5640

Wear rate, frictional temperature, and energy consumption of steel 52100 with different microstructures during sliding

W. LI*
Department of Mechanical Engineering,Changchun University, Changchun, People's Republic of China, 130022; School of Materials Science and Engineering,Harbin Institute of Technology, Harbin, People's Republic of China, 150006
E-mail: wenl@ualberta.ca

Y. WANG, M. F. YAN
School of Materials Science and Engineering,Harbin Institute of Technology, Harbin, People's Republic of China, 150006

Published online: 25 August 2005

In a concerned tribological system, mechanical behavior such as friction and wear, microstructural evolution, and change in environmental temperature impact each other. A complete understanding of these interactions between the above factors is important for a tribological system to function well. In this study, the relationships among the wear rate, the frictional surface temperature, the heat consumption, and the friction energy consumption of steel 52100 with different microstructures during dry sliding were investigated using wear tests and theoretical approaches. The experimental results showed that the wear rate depends strongly on the thermal physical properties of the different microstructures due to their different energy consumptions during sliding. The calculations based on a frictional temperature field model were consistent with the experimental observations.

1. Introduction

Friction and wear of a tribological system are very complicated phenomena and involve various factors such as external forces, material properties, and environmental temperatures. Frictional heating during sliding and the resulting thermal and thermomechanical behavior can play an important role in determining tribological behavior of the system [1, 2]. The high temperature and temperature gradients result in a series of dynamic changes in microstructures and properties of the surface layers, such as tempering softening, phase transformation or even melting; all these phenomena can influence the wear rate [1, 3]. As a result, surface and near-surface temperatures of the sliding layers have been of interest for many years [4, 5]. In order to overcome the difficulties of temperature measurement and the complications of analytical and numerical methods [5, 6], a mathematical model of frictional temperature field has been derived by Wang *et al*. [3]. Based on this model, the temperature field in the surface layer during sliding under various conditions can be predicted. The microstructure and its evolution of a material due to friction between two rubbing components also play an important role in determining wear behavior (e.g., wear resistance). Over the past decades, there has been considerable interest in this issue [7–10]. For example, using thermal techniques and thermal analysis in combination with computer simulations, the transitions in frictional forces and wear rates caused by microstructural changes can be well understood [2, 11, 12]. However, there are almost no reports that concern dynamic wear behavior of materials with different microstructures subjected to a frictional temperature field during sliding wear [13]. This happens partly because there is no simple relationship between original hardness and wear resistance under the conditions of severe wear [3, 10].

It is well known that the friction involves the energy dissipation or the conversion of mechanical work into heat. To study dynamic tribological behavior, it is necessary to understand how the energy associated with mechanical work to overcome the frictional force is converted into heat, resulting in microstructural changes [14, 15]. Therefore, any mechanism that allows for this energy dissipation during sliding deserves consideration, whether it occurs strictly at nominal sliding interfaces or within materials [16]. According to the previous studies [3, 10, 14], the differences in wear

*Author to whom all correspondence should be addressed.
0022-2461
DOI: 10.1007/s10853-005-1508-8

TABLE I Specimen code, heat treatment, microstructure and hardness

Code	Treatment	Microstructure	Hardness (HV)
A	1050°C for 10 min, then 650°C for 30 min, O.Q	Lamellar pearlite	337
B	1050°C for 10 min, aged at 120°C for 24 h after holding at −196°C for 2 h	Martensite	835
C	840°C for 10 min, O.Q., tempered at 160°C for 3 h	Tempered martensite + carbide + retained austenite	772

resistance of the various microstructures were caused by the differences in energy consumption in surface layers during sliding. It is therefore expected that there should be strong relationships among the wear rate, frictional temperature field, and energy consumption during friction and wear of a material with different microstructures.

In this study, based on our previous work [13, 17], steel 52100 was chosen as a typical sample material to investigate tribological behavior induced by sliding using experimental and theoretical approaches.

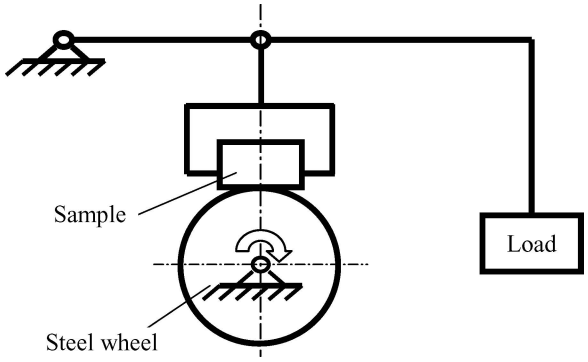

Figure 1 The schematic illustration of a pin-on-ring wear tester.

2. Experimental and theoretical details

2.1. Experimental material and heat treatment

The material used in this study is AISI 52100 steel with composition: 1.01 wt% C, 1.50 wt% Cr, 0.30 wt% Mn, 0.25 wt% Si, 0.02 wt% S and 0.027 wt% P. Pin specimens with dimensions of 10 × 4 × 20 mm were obtained by cutting the plate steel as received. Specimens underwent different heat treatments in order to obtain different microstructures. After heat treatments, all the sample surfaces were first polished using 320 grit sand paper (SiC, particle size: 40 μm) and then using 0.05 μm colloidal silica to get a mirror finish. The polished surfaces were slightly etched with HNO_3 solutions for 5 s in order to remove the deformed layer caused by polishing. The specimens were finally cleaned using an ultrasonic cleaner with reagent grade acetone (for 10 min) and reagent alcohol (for 5 min), and then dried in an inert container for subsequent wear tests. Table I shows the specimen code, heat treatment, microstructure and hardness of pin specimens. Three types of microstructures were obtained after heat treatments, consisting of (A) lamellar pearlite, (B) martensite, and (C) tempered martensite + carbide + retained austenite.

2.2. Wear test

Wear tests were performed on a pin-on-ring tester with rings 40 mm in diameter and 10 mm thick made of hard WC-8% Co material of HRC 75.5 hardness, as illustrated in Fig. 1. The wear surface of the pins was the 10 × 4 mm side. The sliding was along the longitudinal direction. The roughness (Ra) of the contact surface was about 60 μm. All wear tests were carried out at room temperature without lubrication. The test parameters were as follows: normal load 140 N, sliding speed 2 m/s, and sliding distance 600 m. The wear volume of the pin specimens was calculated using weight loss measurements. The wear rate (ϖ) was obtained by using the equation:

$$\varpi = \frac{V}{XL}, \tag{1}$$

where V is the volume loss (mm^3), X is the sliding distance (m), and L is the load (N). The mean value of three measurements was taken as the experimental result.

2.3. Temperature measurement

The temperature distribution of pin specimens was measured with a Probeye 4500 thermal video system. The thermal video pictures can be obtained at a time interval of 0.05 s by means of a real-time recorder in the system. A heat emissivity coefficient of 0.25 was used for the precise temperature measurements.

2.4. A model of frictional temperature field

In general, the temperature distributions of specimen surfaces can be estimated using Ashby's wear maps [18, 19] for a sliding couple over a wide range of load and sliding velocity. However, the estimations based on Ashby's wear maps are approximate, complicated, and, sometimes, dependent on some tunable parameters. In order to overcome the difficulties of temperature measurement and the complications of analytical and numerical methods (also see references [18, 19]), Wang *et al.* [3] proposed a simple model to simulate the temperature field and the bulk surface temperature. In this model, the temperature field in the surface layer during sliding can be expressed by the following equation:

$$T(x,t) = (1 - x/L)f_1(t) + (x/L)f_2(t) - K(t)\sin(\pi/L)x, \tag{2}$$

where T is temperature (K), t is time(s), L is a selected distance constant (m), x is variable distance (m), $f_1(t) = T(0, t)$, $f_2(t) = T(L, t)$, and $K(t) = t^{1/2}/\pi[A_o T_o \exp(-A_o t^{1/2}) + A'_o T'_o \exp(-A'_o t^{1/2})]$, where A_o, A'_o are the constants of material thermal properties and T_o, T'_o are the temperature limits in the moving range. In the present study, we use Equation 2 to calculate the bulk surface temperature.

2.5. Energy consumption during friction and wear

In general, wear of materials can be expressed by wear volume, W. The mechanical work may be measured as the product of the frictional force (F) times the sliding distance (L), i.e., the frictional work is FL. Because F can be easily measured and L is known, the frictional work can be easily calculated. Therefore, as suggested by Wang *et al.* [14], the energy consumption during the friction and wear may be calculated from Equation 3:

$$\varepsilon = (FL)/W = (\mu PL)/W, \tag{3}$$

where μ is the friction coefficient. The values of ε (the unit is J/mm^3) can be called the rate of energy consumption during sliding, which means the energy consumption for the volume (W) of material removed per unit sliding distance (L) under the action of normal load (P).

2.6. Heat consumption during friction and wear

The heat change in a small volume at a given distance x from the frictional surface of the pin specimen should be:

$$\Delta Q_1 = C_p \rho \Delta V (T - T_o), \tag{4}$$

where T is the temperature at x distance/position; T_o is room temperature or initial temperature; ΔV=Adx, where A is the cross-section area or the apparent contact area of the pin specimen; C_p is the specific heat; ρ is density. Therefore, the heat change in the whole pin specimen should be written as:

$$Q_1 = \int_0^L C_p \rho (T - T_o) A dx. \tag{5}$$

3. Results and discussion

3.1. Wear rate

Fig. 2 shows the wear rate of different microstructural pin specimens. It can be seen that there is a considerable difference in the wear rate of various microstructures under the test conditions. The wear rate of different microstructures increased in the following order: lamellar pearlite, martensite, tempered martensite + carbide + retained austenite. It can also be seen that there are no simple relationships between original structural hardness and wear resistance. This also means the microstructure and the hardness of surface layers of the material may be changed due to frictional heating during sliding wear.

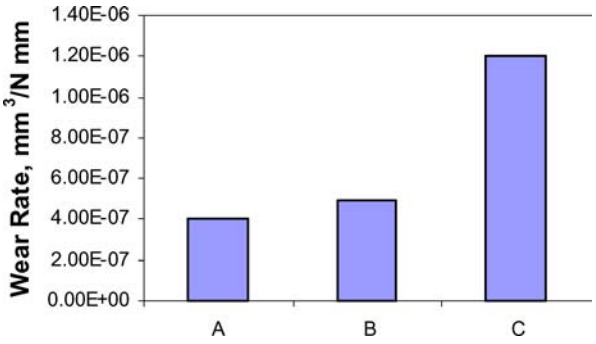

Figure 2 The wear rate of different microstructural pin specimens.

3.2. Frictional surface temperature

If a steady-state temperature distribution is established in the pin specimen, the bulk surface temperature can be calculated by using Equation 2. In order to study the effects of microstructures in surface layers on the frictional temperature field during sliding wear, the bulk surface temperatures of the pin specimens with different microstructures were calculated by Equation 2. Table II shows the calculated temperatures of the wearing surface with different microstructures after 3 min of sliding with 140 N and 2 m/s. The calculated results of the temperature field show that the bulk surface temperatures are 620, 745 and 1340°C for specimens (A), (B) and (C), respectively, as shown in Table II. It was noted [13] that because the different structures possessed different thermal conductivities, the different structures can exhibit different changes in surface temperature, therefore affecting the dynamic processes, for example, the dynamic changes in microstructures, microstresses, and the sizes of mosaic blocks [20].

3.3. Wear rate and frictional surface temperature

Fig. 3 shows the relationship between the wear rates (W_R) and the bulk surface temperatures (T_b) of different microstructural specimens during sliding wear. It can be seen from Fig. 3 that the wear rates of different microstructures are closely related to the temperature fields in the surface layers during sliding. In other words, a higher surface temperature during sliding corresponds to a higher wear rate. As mentioned above, this result is related to the thermal conductivity of the microstructure. Generally, the better the thermal

TABLE II Frictional surface bulk temperatures of steel 52100 with different microstructures after 3 min sliding under the condition of 140 N and 2 m/s

Specimen code	A	B	C
Temperature (°C)	620	745	1340

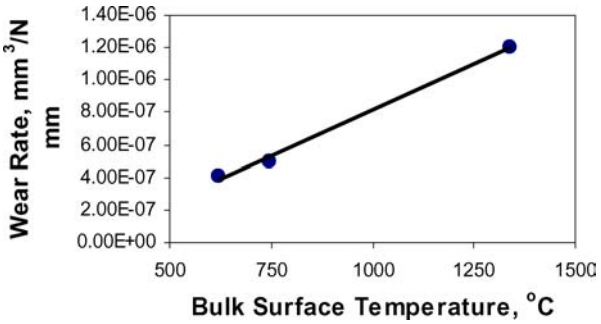

Figure 3 The relationship between the wear rate and the bulk surface temperature.

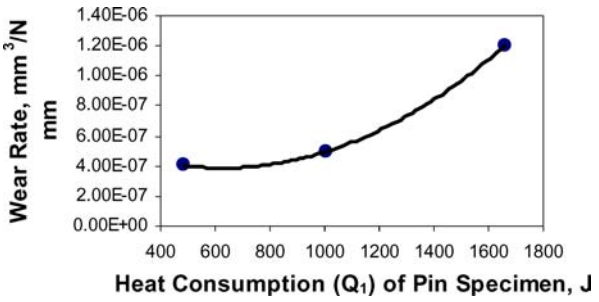

Figure 4 The relationship between the wear rate and the heat consumption of pin specimen.

conductivity, the easier the heat dissipation of the sliding contact surface, and then the lower the temperature rises in the wear surface. Here we present a typical comparison of martensite *vs* pearlite. The energy input for both martensite and pearlite during sliding is basically constant under the same load. However, the energy consumption for the martensite is smaller than that for the pearlite because the thermal conductivity of the martensite (about 79.2 W/m K) is smaller than that of the pearlite (about 87.5 W/m K). As a result, B-type specimens can exhibit the lower wear resistance.

3.4. Heat consumption of pin specimen

According to Wang's model of frictional temperature field [3], the Equation 5 can be written as:

$$\begin{aligned} Q_1 &= \int_0^L C_p \rho \left(T_{(x,t)} - T_o\right) A dx \\ &= C_p \rho A \int_0^L [(1 - x/L) f_1(t) + (x/L) f_2(t) \\ &\quad - K(t) \sin(\pi/L) x - T_o] dx \\ &= C_p \rho A L \{[f_1(t) + f_2(t)]/2 - (1/\pi) K(t) - T_o\}. \end{aligned} \tag{6}$$

Here, let L=1.0 cm. When wear is at the stable-state wear stage, the calculated apparent contact area A is about 40.4 mm^2, and the volume $V = 0.404$ cm^3. The density of the steel is about 7.8 g/cm^3, and the average specific heat C_p is about 0.1546 cal/g·k [21]. Therefore, the heat consumption of the pin specimens with different microstructures in the process can be obtained as shown in Table III. It is therefore found that different microstructural specimens exhibit different heat consumptions during friction and wear due to their different thermal properties.

TABLE III Heat consumption of the pin specimens with different microstructures during sliding under the condition of 140 N and 2 m/s

Specimen code	A	B	C
Heat consumption (J)	485	1004	1660

3.5. Wear rate and heat consumption

Fig. 4 shows the relationship between the wear rate, W_R, and the heat consumption, Q_1, of pin specimens in the process of friction and wear. It can be seen that the wear rate is closely related to the heat consumption during friction and wear. The wear rate increases with increasing heat consumption of the specimens during friction and wear.

3.6. Energy distribution during friction and wear

The total frictional work (μPL) consumed during friction and wear is composed of (1) heat consumption of the pin specimen, Q_1; (2) heat consumption of the ring specimen, Q_2; (3) heat loss in ambient air, Q_3; (4) energy dissipated produce wear debris during sliding, W_1. Therefore, the total frictional work consumed during friction and wear can be expressed as:

$$W_{\text{total}} = Q_1 + Q_2 + Q_3 + W_1. \tag{7}$$

Under a given condition, if Q_1 is higher, Q_2 and Q_3 are also higher, but W_1 is lower. In other words, if the percentage of the total frictional work that is changed into heat is higher, the percentage of the total frictional work which can be used to produce wear would be lower, and vice versa. It is assumed that the heat loss in ambient air, Q_3, can be neglected because it is very small compared with Q_1 and Q_2. The energy dissipation W_1 can be written as:

$$W_1 = \mu PL - (Q_1 + Q_2) \tag{8}$$

where μPL is known, Q_1 can be obtained based on Equation 6. However, it is not easy to obtain the Q_2 because the ring specimen is always undergoing heating and cooling cycling during its rotation. Therefore, the energy dissipation, W_1, could not be easily estimated quantitatively. It can be seen from our previous work [13] that the temperature distribution curves in both pin and ring are almost similar. However, in the present study, the heat emission of the ring is larger than that of the pin, because of the discontinuous contact of the ring during friction and wear. Therefore, a very rough assumption can be made.

$$Q_1 < Q_2. \tag{9}$$

TABLE IV Estimated energy dissipation of steel 52100 with different microstructures during sliding

Specimen code	Assumption	A	B	C
Energy dissipation (J)	If $Q_2 = Q_1$	28430	27392	26080
	If $Q_2 = 2Q_1$	27945	26388	24420

As a qualitative estimation, the energy dissipation, W_1, can be obtained by assuming $Q_1 = Q_2$ or $2Q_1 = Q_2$. The estimated energy dissipation for the different microstructures is shown in Table IV. It can be seen from Tables III and IV that the energy dissipation, W_1, is inversely proportional to the heat consumption Q_1.

3.7. Wear rate and energy consumption

Fig. 5 shows the relationship between the wear rate, W_R, and the energy consumption rate, ε, of different microstructures based on Equation 3. Fig. 6 shows the relationship between the wear rate, W_R, and the wear energy dissipation, W_1, of different microstructures based on the estimated results in Table IV. It can be seen that Figs 5 and 6 have the same tendency. A high wear rate corresponds to a low energy consumption rate or low wear energy dissipation.

3.8. The influence of microstructure on energy consumption

It is suggested [13] that the energy consumption of pearlitic structure may be larger than that of martensitic structure or tempered martensite + carbide + retained austenitic structure, due to the large deformation of the ferrite matrix and the cementite laminae fractures in pearlitic structure. The martensitic structure has high resistance to plastic deformation, and its plastically deformed layer is smaller, thus less energy is consumed for per unit of material removed from martensitic structure than from pearlite. This suggestion can be supported by Fig. 5. It can be seen that the energy consumption during friction and wear is in agreement with the wear rate. The larger the energy consumption rate during sliding, the better the wear resistance of the structure. If a microstructure has a high work hardening exponent, fracture toughness and thermal stability, it may consume greater energy during sliding wear and exhibit higher wear resistance during wear. This indicates that the energy dissipated during friction and wear depends not only on the strength of the surface layers affected by wear, but also on the structural changes in the layers produced by the tribological process. It is known that the pearlitic structure has high plastic deformation ability, fracture toughness, and high thermal conductivity and thermal stability [10]. Therefore, the pearlitic structure can reach a relatively lower frictional surface temperature and exhibit a good wear resistance, as shown in Fig. 3. In contrast to pearlitic structure, martensitic structure can exhibit a high frictional surface temperature and a poor wear resistance due to its low plastic deformation ability and thermal conductivity.

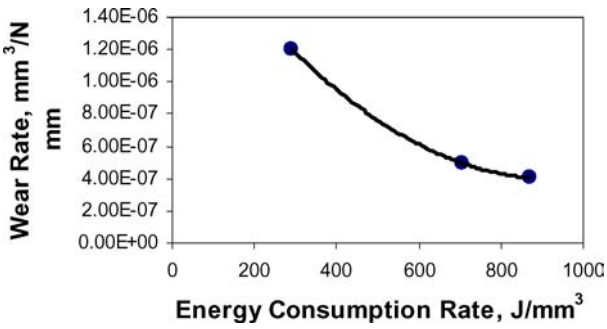

Figure 5 The relationship between the wear rate and the energy consumption rate.

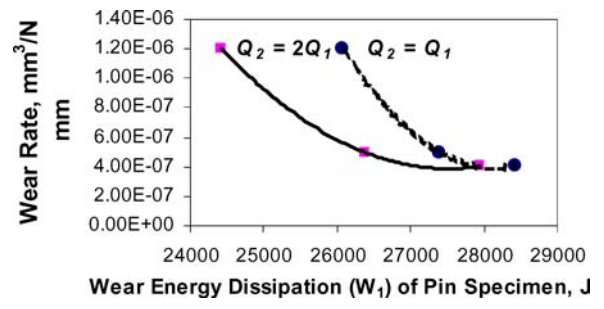

Figure 6 The relationship between the wear rate and the wear energy dissipation of pin specimen.

4. Conclusion

Research has been conducted to investigate the tribological behavior and various microstructures in steel 52100 during sliding. It is demonstrated that the wear rate of the steel depends strongly on the thermal physical properties of the microstructures that exhibit completely different heat consumption or frictional surface temperatures. A higher heat consumption or surface temperature during sliding corresponds to a higher wear rate. Furthermore, for a microstructure, the larger the wear energy dissipation, the better the wear resistance.

References

1. S. C. LIM and M. F. ASHBY, *Acta Metall.* **35** (1987) 1.
2. T. F. J. QUINN, *Wear* **153** (1992) 179.
3. Y. WANG, T. C. LEI, M. F. YAN and C. Q. GAO, *J Phys. D: Appl. Phys.* **25** (1992) A165.
4. H. CZICHOS, "Tribology" (Elsevier, Amsterdam, 1992).
5. F. E. JR. KENNEDY, *Wear* **100** (1984) 453.
6. K. KNOTHE and S. LIEBELT, *ibid.* **189** (1995) 91.
7. D. A. RIGNEY and W. A. GLAESER, "Wear of Materials" (ASME, New York, 1977) p. 41.
8. K. H. ZUM-GAHR, "Microstructures and Wear of Materials" (Elsevier, Amsterdam, 1987).
9. J. KALOUSEK, K. M. FEGREDO and E. E. LAUFFR, *Wear* **105** (1985) 199.
10. Y. WANG, L. PAN and T. C. LEI, *ibid.* **143** (1991) 57.
11. N. C. WELSH, *Phil. Trans. R. Soc. Ser. A* **257** (1965) 31.
12. *Idem., ibid.* **257** (1965) 51.
13. Y. WANG, M. F. YAN, X. D. LI and T. C. LEI, *Trans. ASME J. Tribol.* **116** (1994) 255.
14. Y. WANG, M. MCNALLAN, X. ZHANG and T. C. LEI, *Scripta Mater.* **36** (1997) 213.
15. M. O. ROBBINS and J. KRIM, *MRS Bulletin* **23**(6) (1998) 23.
16. D. A. RIGNEY and L. E. HAMMERBERG, *ibid.* **23**(6) (1998) 32.

17. Y. WANG, X. D. LI and Z. C. FENG, *Scripta Mater.* **33** (1995) 1163.
18. M. F. ASHBY and S. C. LIM, *Scr. Metall. Mater.* **24** (1990) 805.
19. M. F. ASHBY, J. ABULAWI and H. S. KONG, *Tribology Trans.* **34** (1991) 577.
20. Y. WANG, X. L. SUN, S. L. XU and J. J. LIU, *Wear* **162–164** (1993) 183.
21. Y. S. TOULOUKIAN, "Thermophysical Properties of Matter, The TPRC Data Series," Specific Heat (IFI/Plenum, New York-Washington, 1970)) Vol. 4.

Received 12 January
and accepted 14 April 2005